RAPID COMMUNICATIONS

PHYSICAL REVIEW B VOLUME 48, NUMBER 18 1 NOVEMBER 1993-II

Infrared reflectivity of $La_{1.89}Ca_{1.11}Cu_2O_{6\pm\delta}$ single crystals at various O_2 annealing pressures

H. Shibata, T. Watanabe, K. Kinoshita, A. Matsuda, and T. Yamada
NTT Basic Research Laboratories, Musashino, Tokyo 180, Japan
(Received 12 July 1993; revised manuscript received 26 August 1993)

The *ab*-plane reflectivity of $La_{1.89}Ca_{1.11}Cu_2O_{6\pm\delta}$ single crystals, whose properties change from semiconductor to superconductor under high-oxygen-pressure annealing, is measured between 250 and 20 000 cm $^{-1}$ at room temperature. Although the annealing increases the oxygen content very slightly, the spectra change in the same way as seen in other cuprates with carrier doping: a charge-transfer peak disappears and low-energy excitation increases. We suggest the possibility that holes in the apex oxygen redistribute to the CuO_2 planes. Mid-infrared absorption is observed in all samples. Relation between the mid-infrared absorption and the influence of La and Ca disorder on the CuO_2 planes is also discussed.

Although there has been disagreement about how to interpret the non-Drude optical behavior of high-T_c cuprates,[1] the essential feature of the optical spectrum is brought about with carrier doping into the CuO_2 planes. In the case of $La_{2-x}Sr_xCuO_4$,[2] the spectral weight of the Cu-O charge-transfer (CT) gap is transferred to the Drude-type absorption and the mid-infrared absorption peaks, and the center of the mid-infrared peak shifts toward zero frequency with carrier doping. These changes also hold for the other high-T_c cuprates, such as $Nd_{2-x}Ce_xCuO_4$, $Pr_{2-x}Ce_xCuO_4$, and $Bi_2Sr_2Ca_{1-x}(Y, Nd)_xCu_2O_8$.[1-4] However, $YBa_2Cu_3O_{7-\delta}$ is the exceptional case. Although similar changes are observed in the twinned $YBa_2Cu_3O_{7-\delta}$ crystal,[5] polarized measurements of the twin-free $YBa_2Cu_3O_{7-\delta}$ crystal reveal that the mid-infrared peak is associated with the chains and there is no manifest mid-infrared absorption peak associated with the CuO_2 planes, even at low doping (T_c=60 K).[6,7] So, it is interesting to investigate whether this feature of $YBa_2Cu_3O_{7-\delta}$, which gives strong support to the one-component theory,[6,7] is specific for a pair of pyramidal Cu-O planes. Because $La_{1.89}Ca_{1.11}Cu_2O_{6\pm\delta}$ has only a pair of pyramidal Cu-O planes facing each other and no chains, study of this system shows the relationship between this feature and the pyramidal structure, and hence some insight into the generality of the one-component theory. In an earlier report by Kaplan *et al.*,[8] the mid-infrared absorption peak is observed in $La_2SrCu_2O_{6\pm\delta}$ nonsuperconducting ceramics. However, to our knowledge no precise measurements on single crystals have been reported.

$La_{1.89}Ca_{1.11}Cu_2O_{6\pm\delta}$ shows superconductivity only when annealed under high oxygen pressure above 100 atm,[9] but the effects of such annealing are not clear. Neutron and x-ray diffraction studies and chemical analysis of sintered $La_{2-x}Ca_{1+x}Cu_2O_{6\pm\delta}$ show very little change in oxygen content between superconducting and nonsuperconducting samples.[10-12] One may think that the metal-insulator transition is due to a sort of strong localization, since there exist random potentials due to La and Ca disorder and oxygen vacancies adjacent to the CuO_2 planes. In this case, a small increase in carriers is sufficient to promote the transition. However, recent transport measurements of single-crystal $La_{1.89}Ca_{1.11}Cu_2O_{6\pm\delta}$ show that the transition from nonsuperconducting (20 atm) to superconducting (100 atm) is mainly due to an increase in the hole concentration, although the increase in T_c in samples annealed at 300 atm O_2 versus 100 atm mainly results from a reduction in the impurity scattering.[9]

The present paper reports measurements of the *ab*-plane reflectivity of $La_{1.89}Ca_{1.11}Cu_2O_{6\pm\delta}$ single crystals annealed at various oxygen pressures. The spectra show that carriers are doped into the CuO_2 plane at increased annealing pressure. We discuss this change in comparison with results from transport and neutron experiments and Madelung potential calculation. Mid-infrared absorption is observed in all samples. We also discuss the relation between this absorption and the influence of La and Ca disorder on the CuO_2 planes.

The sample preparation method and transport properties have been described in detail in previous papers.[9,13] Single crystals of $La_{1.89}Ca_{1.11}Cu_2O_{6\pm\delta}$ were synthesized in air via a CuO flux method, and annealed at various oxygen pressures for 200 h using a furnace for hot isostatic pressing (HIP). Although the as-grown and the 20-atm-O_2-annealed samples do not show superconductivity down to 4 K, the 100-atm-O_2-annealed sample showed a metallic conductivity and showed a T_{c0} of 13 K, and the 300-atm-O_2-annealed sample showed a T_{c0} of 40 K. The bulk single crystallinity was confirmed from an x-ray precession photograph.

Room-temperature reflectivity measurements were carried out in a frequency range between 250 and 20 000 cm^{-1} using a rapid scan interferometer combined with a Spectra-Tech IR-PLAN microscope. Typical focus spot size was 0.7 mm × 0.7 mm. The accuracy of the measurement system is confirmed by comparing the reflectivity spectrum of a $YBa_2Cu_3O_{7-\delta}$ crystal with those previously obtained.[5,14] Although the surface of the as-grown crystal was shiny, it was damaged by O_2-HIP annealing, so we polished the surfaces with Al_2O_3 powder with a grain size of 0.3 μm.

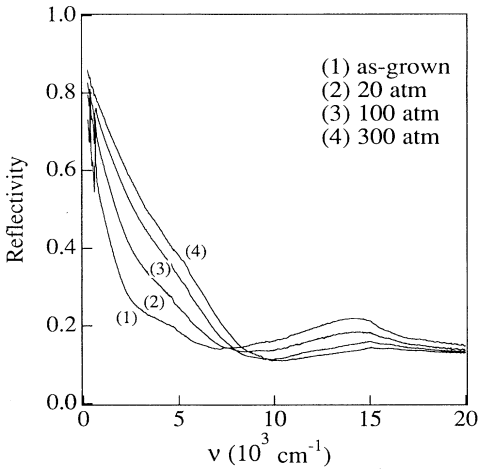

FIG. 1. Reflectivity spectra ($\mathbf{E}\perp c$) of $La_{1.89}Ca_{1.11}Cu_2O_{6\pm\delta}$ single crystals for various oxygen pressures during annealing.

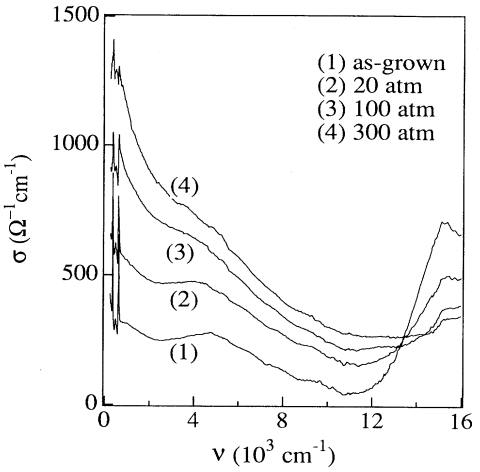

FIG. 2. Optical conductivity of $La_{1.89}Ca_{1.11}Cu_2O_{6\pm\delta}$ single crystals for various oxygen pressures during annealing obtained from the Kramers-Kronig transformation of the reflectivity spectra ($\mathbf{E}\perp c$).

Figure 1 shows the *ab*-plane reflectivity of $La_{1.89}Ca_{1.11}Cu_2O_{6\pm\delta}$ single crystals annealed at various oxygen pressures. It shows many features that have been found to accompany the progression from insulator to superconductor with carrier doping in other cuprates.[1–4] The reflectance of the as-grown sample is characterized by two strong phonons at 360 and 643 cm^{-1}; rather low reflectivity in the mid-infrared region; and a peak due to the Cu-O charge-transfer excitation near 15 000 cm^{-1}. Growth in the reflectance at low frequencies indicates that carriers are already present even in the as-grown sample, although it is semiconducting $[d\rho_{ab}/dT(300\ \mathrm{K}) < 0]$. With increasing oxygen annealing pressure, the reflectivity of the CT peak decreases, and the reflectivity edge at about 8000 cm^{-1} becomes sharp but does not shift. The reflectivity drops with frequency in nearly linear fashion in the 300-atm-O_2 sample. Optical phonons are not completely screened even in this sample, suggesting the low doping of carriers.

These changes become clearer when the reflectivity spectrum is converted to the optical conductivity by a Kramers-Kronig transformation. In transforming the spectrum, we use a Hagen-Rubens extrapolation for low frequency and La_2CuO_4 data by Tajima *et al.*[15] for high frequency. The Hagen-Rubens extrapolation gives a smooth connection and the extrapolated dc conductivity agreed with transport measurement values for the 100- and 300-atm-O_2 samples. The extrapolated conductivity $\sigma(\omega \sim 0)$ was about 900 $\Omega^{-1}cm^{-1}$ for the 100-atm-O_2 sample and 1400 $\Omega^{-1}cm^{-1}$ for the 300-atm-O_2 sample by IR measurement, while the resistivity measurements give $\sigma(300\ \mathrm{K}) \sim 600\ \Omega^{-1}cm^{-1}$ and 1200 $\Omega^{-1}cm^{-1}$, respectively. This extrapolation gives higher conductivity than transport values for the 20-atm-O_2 and the as-grown samples. These higher values may be due to the unscreened phonons below 250 cm^{-1}, but the effect is negligible for the following discussion. The choice of high-frequency extrapolation affects the magnitude of the conductivity below 20 000 cm^{-1}, especially the oscillator strength of the CT excitation. We use this extrapolation because some of the interband excitations of $La_{1.89}Ca_{1.11}Cu_2O_{6\pm\delta}$, such as excitation from the O $2p$ valence bands to the conduction bands of La $5d, 4f$ orbitals, may be found by using the spectrum of La_2CuO_4.

Figure 2 shows the optical conductivity of these samples. The spectral weight of the CT excitation decreases and the mid- and far-infrared regions rapidly increase with increase of the oxygen annealing pressure. Clearly, $\sigma(\omega)$ has two components, a peak at $\omega = 0$ and the broad peak centered at the mid-infrared region. The mid-infrared peak slightly shifts to lower frequencies as its strength increases. These changes are typical for high-T_c superconductors with carrier doping and suggest that carriers are doped in the CuO_2 planes by high-oxygen-pressure annealing. Since $La_{1.89}Ca_{1.11}Cu_2O_{6\pm\delta}$ has tetragonal symmetry and no chain, these characteristics are intrinsic to the CuO_2 planes. The existence of the mid-infrared peak in $La_{1.89}Ca_{1.11}Cu_2O_{6\pm\delta}$ indicates that the absence of the mid-infrared peak observed in the $YBa_2Cu_3O_{7-\delta}$ is not unique for the pyramidal Cu-O planes. We suggest the mid-infrared peak may be related to the influence of cation disorder on the CuO_2 planes, which is discussed later.

The increase in carriers by high-oxygen-pressure annealing is clearly shown in Fig. 3, which displays the integrated spectral weight given as

$$N^*_{\mathrm{eff}}(\omega) = \frac{2m_eV}{\pi e^2}\int_0^{\omega}\sigma_1(\omega')d\omega',$$

where m_e is the bare electron mass and V is the volume of the unit cell. The integrated spectral weight below 10 000 cm^{-1} is 0.26 for the as-grown sample and 0.83 for the 300-atm-O_2 sample, which means 0.065 and 0.21 carriers per one CuO_2 unit, respectively, assuming $m^* = m_e$. Such a large increase in N^*_{eff} is comparable with the carrier concentration increase estimated by Hall coefficient measurement: the $1/eR_H$ of the 300-atm-O_2 sample is about ten times larger than that of the as-grown sample.[9] On the other hand, the increase in the total carrier concen-

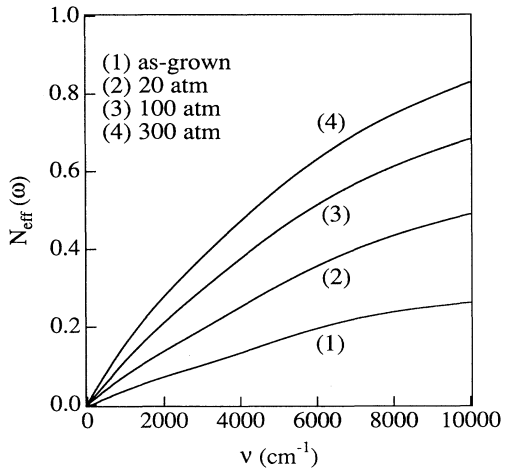

FIG. 3. Integrated spectral weight of $La_{1.89}Ca_{1.11}Cu_2O_{6\pm\delta}$ single crystals for various oxygen pressures during annealing.

tration, determined by the chemical and structural analysis, is very small.[10,11] Although we did not determine the oxygen content for this crystal, neutron diffraction measurement of sintered $La_{1.82}Ca_{1.18}Cu_2O_{6\pm\delta}$ samples shows oxygen content of 5.99 ± 0.02 for a nonsuperconducting (2 atm) sample and 6.014 ± 0.017 for a superconducting (400 atm) one. Assuming the same oxygen content for the present case would mean 0.045 and 0.069 carriers per CuO_2 unit, for the as-grown and the 300-atm-O_2 samples, respectively. The large increase in $N_{\rm eff}^*$ and the small increase in the oxygen content due to high-pressure annealing suggest that carriers are initially located in orbitals where the optical excitation is forbidden for the light polarized parallel to the CuO_2 plane, such as the apex O $2p_z$ orbitals for nonsuperconducting samples. They moved into the CuO_2 plane for superconducting samples. These changes are different from what is expected for the nonsuperconducting to superconducting transition due to the localization of the carrier in the CuO_2 plane. In this case, no integrated spectral weight change is expected at room temperature, although localized carriers may cause absorption peaks in the far-infrared region at low temperature.

It has been pointed out that the capability of the hole doping into the CuO_2 plane is strongly related to the difference in Madelung energy ΔV_A, between the apex oxygen and the plane oxygen.[16,17] Using the neutron data,[11] ΔV_A is calculated to be -0.6 eV for nonsuperconducting samples, and -0.26 eV for superconducting ones.[18] The reduction of $|\Delta V_A|$, which is mainly due to slight oxygen intercalation between two CuO_2 planes and increased ordering of La and Ca sites, means carriers are more favored to be doped in the apical oxygen site for the nonsuperconducting sample than for the superconducting sample. This is consistent with our suggestion.

In Fig. 3, $N_{\rm eff}^*$ is much larger than the total carrier concentration n. This large spectral weight is also observed in lightly doped $La_{2-x}Sr_xCuO_{4\pm\delta}$ and $Pr_{2-x}Ce_xCuO_{4\pm\delta}$,[2,3] but in lightly doped $YBa_2Cu_3O_{6+\delta}$, $N_{\rm eff}^* \sim n$.[6,7] This difference might not be due simply to the difference in effective mass. Since large mid-infrared absorption is observed in the former cases but not in the latter case, their excess spectral weights may be related to the mid-infrared absorption band. It is interesting to point out that in the former cases, there always exist random orderings of cations and/or oxygen vacancies adjacent to the CuO_2 planes. The random potential due to these cations may influence the electronic character of CuO_2 planes, and may cause the mid-infrared absorption, similarly as it does in an impure semiconductor,[7,19,20] although the position of the absorption peak is much higher than that in semiconductors. The influence of random potential on the CuO_2 planes is not yet well understood.

Although the nonsuperconducting to superconducting transition is mainly due to the redistribution of carriers into the CuO_2 planes, the transport measurement suggests that the dominant effect of T_c increase due to the high-oxygen-pressure annealing between 100 and 300 atm is to reduce disorder. To compare this with our results, we fit the conductivity of the 100- and 300-atm-O_2 samples below 8060 cm^{-1} by one Drude term and four Lorentz (two for phonons and two for mid-infrared absorption) terms. We adopt two Lorentz terms for the mid-infrared absorption because a fit by one Lorentz term gives an unphysically large scattering rate for the Drude carriers, and a fit by more than three Lorentz terms gives large ambiguity. The result shows $\omega_p = 5036$ cm^{-1}, $\tau^{-1} = 445$ cm^{-1}, $\omega_{p_1} = 752$ cm^{-1}, $\tau_1^{-1} = 53$ cm^{-1}, $\omega_1 = 363$ cm^{-1}, $\omega_{p_2} = 1117$ cm^{-1}, $\tau_2^{-1} = 96$ cm^{-1}, $\omega_2 = 665$ cm^{-1}, $\omega_{p_3} = 9293$ cm^{-1}, $\tau_3^{-1} = 2220$ cm^{-1}, $\omega_3 = 1013$ cm^{-1}, $\omega_{p_4} = 14\,408$ cm^{-1}, $\tau_4^{-1} = 7437$ cm^{-1}, and $\omega_4 = 4268$ cm^{-1} for the 100-atm-O_2 sample and $\omega_p = 4673$ cm^{-1}, $\tau^{-1} = 246$ cm^{-1}, $\omega_{p_1} = 675$ cm^{-1}, $\tau_1^{-1} = 55$ cm^{-1}, $\omega_1 = 364$ cm^{-1}, $\omega_{p_2} = 809$ cm^{-1}, $\tau_2^{-1} = 138$ cm^{-1}, $\omega_2 = 635$ cm^{-1}, $\omega_{p_3} = 11\,941$ cm^{-1}, $\tau_3^{-1} = 2332$ cm^{-1}, $\omega_3 = 765$ cm^{-1}, $\omega_{p_4} = 14\,785$ cm^{-1}, $\tau_4^{-1} = 7711$ cm^{-1}, and $\omega_4 = 4591$ cm^{-1} for the 300-atm-O_2 sample, where ω_p and τ^{-1} are the plasma frequency and scattering rate for the Drude carriers, and ω_{p_i}, τ_i^{-1}, and ω_i are the strength, scattering rate, and center of ith Lorentz term. The large reduction of scattering rate and constancy of plasma frequency in the Drude term are consistent with the results of the transport measurement.

In conclusion, we have measured the reflectivity of $La_{1.82}Ca_{1.18}Cu_2O_{6\pm\delta}$ single crystals, whose properties change from semiconductor to superconductor for various O_2 pressures during annealing. The spectra change in the same way as seen in other cuprates with carrier doping. The mid-infrared absorption peak is observed and may be related to the La and Ca disorder potentials. We suggest that the spectra change due to the carrier redistribution from apex O $2p_z$ to CuO_2 planes. Finally reduction of scattering rate is observed from the 100- to the 300-atm-O_2 samples.

We would like to thank Professor S. Uchida and Dr. T. Arima at Tokyo University for their preliminary measurements. We would also like to thank Dr. A. Yamashita for his help in the infrared measurement, Dr. H. Koizumi for his Madelung energy calculation, and K. Semba for his $YBa_2Cu_3O_{7-\delta}$ crystal.

[1] D. B. Tanner and T. Timusk, in *Physical Properties of High Temperature Superconductors III,* edited by D. M. Ginsberg (World Scientific, Singapore, 1992).
[2] S. Uchida, T. Ido, H. Takagi, T. Arima, Y. Tokura, and S. Tajima, Phys. Rev. B **43**, 7942 (1991).
[3] S. L. Cooper, G. A. Thomas, J. Orenstein, D. H. Rapkine, A. J. Millis, S-W. Cheong, A. S. Cooper, and Z. Fisk, Phys. Rev. B **41**, 11 605 (1990).
[4] I. Terasaki, T. Nakahashi, S. Takebayashi, A. Maeda, and K. Uchinokura, Physica C **165**, 152 (1990).
[5] J. Orenstein, G. A. Thomas, A. J. Millis, S. L. Cooper, D. H. Rapkine, T. Timusk, L. F. Schneemeyer, and J. V. Waszczak, Phys. Rev. B **42**, 6342 (1990).
[6] L. D. Rotter, Z. Schlesinger, R. T. Collins, F. Holtzberg, C. Field, U. W. Welp, G. W. Crabtree, J. Z. Liu, Y. Fang, K. G. Vandervoort, and S Fleshler, Phys. Rev. Lett. **67**, 2741 (1991).
[7] S. L. Cooper, D. Reznik, A. Kotz, M. A. Karlow, R. Liu, M. V. Klein, W. C. Lee, J. Giapintzakis, D. M. Ginsberg, B. W. Veal, and A. P. Paulikas, Phys. Rev. B **47**, 8233 (1993).
[8] S. G. Kaplan, T. W. Noh, P. E. Sulewski, H. Xia, A. J. Sievers, J. Wang, and R. Raj, Phys. Rev. B **38**, 5006 (1988).
[9] T. Watanabe, K. Kinoshita, and A. Matsuda, Phys. Rev. B **47**, 11 544 (1993).
[10] K. Kinoshita, H. Shibata, and T. Yamada, Physica C **176**, 433 (1991).
[11] K. Kinoshita, F. Izumi, T. Yamada, and H. Asano, Phys. Rev. B **45**, 5558 (1992).
[12] K. Kinoshita, H. Shibata, and T. Yamada, Physica C **171**, 523 (1990).
[13] T. Ishii, T. Watanabe, K. Kinoshita, and A. Matsuda, Physica C **179**, 39 (1991).
[14] Z. Schlesinger, R. T. Collins, F. Holtzberg, C. Feild, G. Koren, and A. Gupta, Phys. Rev. B **41**, 11 237 (1990).
[15] S. Tajima, H. Ishii, T. Nakahashi, T. Takagi, S. Uchida, M. Seki, S. Suga, Y. Hidaka, M. Suzuki, T. Murakami, K. Oka, and H. Unoki, J. Opt. Soc. Am. B **6**, 475 (1989).
[16] J. Kondo, Y. Asai, and S. Nagai, J. Phys. Soc. Jpn. **57**, 4334 (1988).
[17] Y. Ohta, T. Tohyama, and S. Maekawa, Phys. Rev. B **43**, 2968 (1991).
[18] F. Izumi, in *The Rietveld Method,* edited by R. A. Young (Oxford Univ. Press, Oxford, 1993).
[19] G. A. Thomas, D. H. Rapkine, S. L. Cooper, S-W. Cheong, A. S. Cooper, L. F. Schneemeyer, and J. V. Waszczak, Phys. Rev. B **45**, 2474 (1992).
[20] G. A. Thomas, M. Capizzi, F. DeRosa, R. N. Bhatt, and T. M. Rice, Phys. Rev. B **23**, 5472 (1981).